

Characterization of hybrid HIT solar cells based on a hole selective MoO_x contact

Nicolás Mateos Estévez, Denis Pascual, and Jordi Sastre-Pellicer
Engineering Physics Projects II - Polytechnic University of Catalonia (BarcelonaTech)

I. OBJECTIVES

The aim of this project is to study the behavior of HIT solar cells with an ultrathin layer of molybdenum oxide (MoO_x) as a transparent hole selective contact to n-type silicon. Current-voltage and capacitance-voltage characteristics will be studied and a circuital model for this kind of solar cells will be presented.

II. ADVANTAGES OF HYBRID HIT SOLAR CELLS

Heterojunction with Intrinsic Thin layer (HIT) solar cells are an improvement of the classic solar cells, providing a higher efficiency. All the upgrades that HIT cells provide have the aim to improve the path that the charge carriers have to travel. That involves improving the recombination in the device interfaces. To achieve this, HIT solar cells include a thin film of hydrogenated amorphous silicon instead of directly doping the crystalline silicon of the wafer.

Classical solar cells are fabricated starting from the crystalline silicon wafer and diffusing the dopant material on it. This process consists on evaporating the dopant material from a wafer previously prepared and waiting until it condenses on the silicon wafer. Then the dopant wafer is removed and the dopant material, that has been deposited on the silicon wafer, has to diffuse deeper into it. This requires temperatures of 1000°C and lasts around 20-30 min. HIT solar cells improve this issue by adding an amorphous silicon doped film at temperatures below 300°C . However this process can be optimized because it still requires high vacuum chambers and the preparation of amorphous silicon, which requires the use of dangerous gasses and therefore specialized equipment.

The fabrication process of classical HIT solar cells is a drawback that hybrid cells can improve. The idea is to replace the amorphous silicon p-type film, that acts as an emitter, by an organic semiconductor able to acquire the same role. For this project, molybdenum oxide was used as a p-type emitter deposited on a n-type crystalline silicon wafer with the aim of obtaining the same structure but economizing the fabrication process. The advantage is that MoO_x can be evaporated easily even though it still takes place in vacuum. However, improvements in which vacuum conditions are not required are being studied.

III. PARTS OF A HYBRID HIT SOLAR CELL

A typical hybrid solar cell based on MoO_x is made up of [1]:

- A n-doped wafer of crystalline silicone of $280\ \mu\text{m}$.

- A MoO_x interlayer used as a transparent hole selective contact to n-type silicon. One of the topics that are discussed in this article is the change in the performance of the solar cell depending on the thickness of this interlayer.
- An optional ultra thin intrinsic a-Si:H layer between the wafer and the MoO_x layer to improve surface passivation.
- An anode made of a 70 nm layer of ITO with a grid of silver contacts.
- A cathode made of aluminium with a thin layer of hydrogenated amorphous silicon in contact with the silicon wafer. Several laser microperforations in the electrode allow the amorphous silicon to drive the dopant into the underlying silicon to create a shallow, highly doped n+ emitter region. This process improves considerably the conductivity [3].

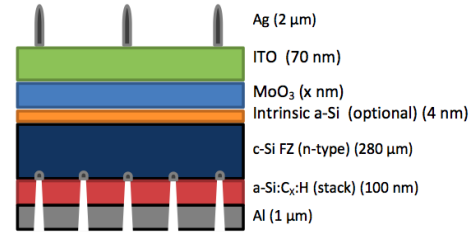


FIG. 1. $\text{MoO}_x/\text{a-Si:H}/\text{c-Si}$ HIT solar cell structure

IV. CURRENT-VOLTAGE CHARACTERISTICS

The main idea of this analysis is to measure the intensity that goes through the solar cell while the voltage is changed [4].

For both the Hybrid HIT solar cells and the Schottky diodes, the results have got similarities with the ones for a diode.

The current-voltage characteristics of the solar cell junction with parasitic resistances at forward bias are represented by the equation:

$$I = I_0 \left(\exp \left[\frac{q}{nk_B T} (V - R_s I) \right] - 1 \right) + \frac{V - I R_s}{R_p} \quad (1)$$

The series resistance R_s accounts for ohmic losses due to the bulk resistance of the semiconductor material and the metallic contacts. Current leakages across the junction are represented by the shunt resistance R_p . The ideality factor n provides information on the quality of

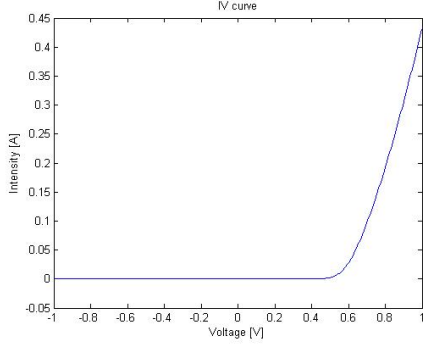


FIG. 2. The diode behaviour of the Hybrid Solar cell with a 10nm MoO_3 layer

the junction and the saturation current I_0 is related to the properties of the semiconductor material [5].

There are three main regions when the logarithm of the intensity is plotted versus the voltage.

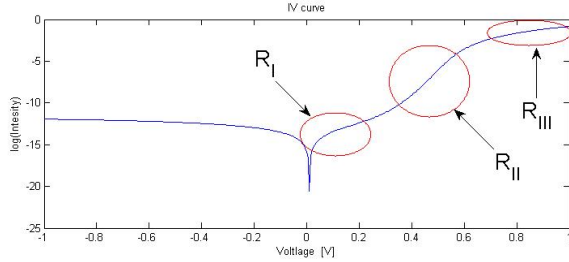


FIG. 3. Plot of the $\log(I)$ -V, and the three regions of interest are marked (R_I , R_{II} and R_{III})

From region R_I one can extract R_p . This resistance is in fact obtained from the plot of the intensity vs. the voltage. The following expression must hold:

$$R_p = \left. \frac{dV}{dI} \right|_{V=0} \quad (2)$$

The parameters have been obtained using numerical methods, by doing an approximation of the slope of the IV curve and obtaining its inverse. The results for the different devices studied are the following:

	Al diode	Au diode	HIT 10nm	HIT 20 nm	HIT 30nm
R_p	30.40 $k\Omega$	17.35 $k\Omega$	58.17 $k\Omega$	36.76 $k\Omega$	48.61 $k\Omega$

The values correspond to two different MoO_3 Schottky diodes, one with an aluminium electrode and the other one with a gold electrode, and to three hybrid HIT solar cells with different thicknesses of the MoO_3 layer.

From region R_{II} one can obtain two main parameters: the ideality factor, n , and the reverse saturation current, I_0 . Taking into account that this second region fits with the behaviour of a diode, one must recall the expression of the diode and proceed to isolate I_0 and n .

$$I = I_0 \left(\exp\left(\frac{V - R_s I}{n \frac{k_B T}{q}}\right) - 1 \right) \quad (3)$$

In order to take into consideration the region where the study is taking place, $V \gg R_s I$. Applying natural logarithms to (3) and taking into account the simplification, one obtains: $\log(I) = \log(I_0) + \frac{V}{nV_t}$. Therefore if the data obtained are fitted into a function of the form $f(x) = p_1 x + p_2$, then $p_1 = \frac{1}{nV_t}$ and $p_2 = \log(I_0)$. The following results were obtained:

	Al diode	Au diode	HIT 10nm	HIT 20 nm	HIT 30nm
I_0	11.36 nA	27.10 nA	67.25 nA	0.37 nA	62.08 nA
n	1.674	1.510	1.332	1.312	1.373

Finally from region R_{III} the value of R_s can be obtained. Considering the ideal curve of the diode and subtracting it to the obtained one, one can obtain the value of the series resistance. From equation (3), one gets that: $\log(I) - \log(I_{\text{ideal diode}}) = -R_s I / nV_t$. And thus:

$$R_s = \frac{-nV_t(\log(I) - \log(I_{\text{ideal diode}}))}{I} \quad (4)$$

	Al diode	Au diode	HIT 10nm	HIT 20 nm	HIT 30nm
R_s	8 Ω	2.62 Ω	0.72 Ω	0.86 Ω	0.66 Ω

Parallel measurements have been done but with a light source of $0.1W/cm^2$ over the hybrid HIT solar cell. When the IV curve is measured with light, it appears lower than the one in darkness due to photogenerated current. In the region where $I < 0$ and $V > 0$, an output power can be obtained from the solar cell.

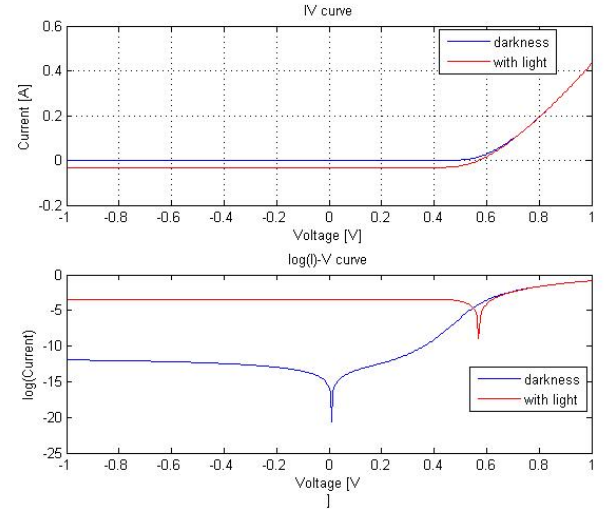


FIG. 4. For the first plot: The intersection of the Light curve with the y axis (i.e. $V = 0$) gives the I_{sc} and the intersection point with the x axis (i.e. $I = 0$) gives the V_{oc} . Plot of the $\log(I)$ measured in the darkness and with a light source of $0.1W/cm^2$

Taking the point of maximum power of the curve, the efficiency of the solar cell can be obtained.

	HIT 10nm	HIT 20nm	HIT 30nm
η	13.73 %	13.72 %	12.19 %

V. CAPACITANCE-VOLTAGE CHARACTERISTICS

A. Capacitance-voltage curves

In a simple solar cell, in the dark, the response to an applied voltage can be modelled as a diode with a given capacitance.

This capacitance is due to the charge accumulated in the space charge region of the PN junction, and this charge depends on the applied voltage, so there are a relation between the capacity and the voltage [6].

$$\frac{1}{C^2} = \frac{2(V_{bi} - V)}{\epsilon q N_d A^2} \quad (5)$$

Although the modifications that HIT solar cells provide, the relation capacitance - voltage remains the same. The unknown is what happens with the substitution of the amorphous silicon emitter by the molybdenum oxide. The impedance of a molybdenum oxide hybrid solar cell has been measured in order to find it out. The issue is that with this change, it is not clear what is happening in the interface between the emitter and base. The idea is to measure the impedance of the device and how it evolves with respect to different parameters, then an approximated circuital model could be found out and from it, infer the physical process that are coming about. The applied mean voltage and the frequency of the time-variant voltage signal are two parameters that allowed the measurement of the impedance.

A previous study of Schottky diodes was done before proceeding with the characterization of the MoO_x hybrid HIT solar cells. These two devices just differ in an ITO layer and metal layer that the hybrid HIT solar cells has instead of a metallic lattice as Schottky diodes have. The aim of the study of the Schottky diodes is to see if changing the metal of the metallic contacts influences the measurements. According to a common diode, $1/C^2$ follows the expression of Equation (5). The measures are the following:

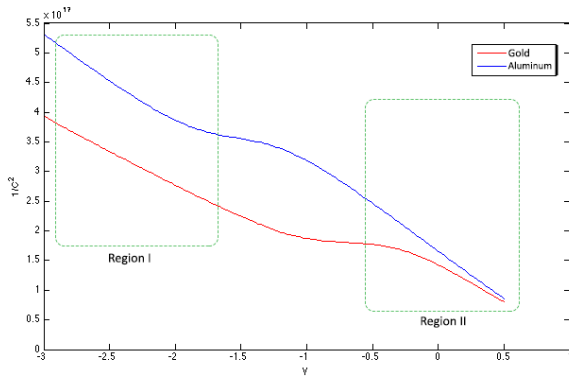


FIG. 5. $1/C^2$ plot of the Schottky diodes at 1 MHz

For both Schottky diodes the function $1/C^2$ are non-linear, unlike it was expected according to Equation (5). It is observed that in both plots there are two linear regions separated by a step. At high inverse voltages the linear behaviour is similar to the expected one, but from the step to low voltages the measures do not add up with the classical behaviour. From *Region 1* and *Region 2*, the theoretical values of V_{bi} and N_d have been calculated by using Equation (5).

Aluminum		Gold	
Region 1	Region 2	Region 1	Region 2
$V_{bi} = 0.84V$	$V_{bi} = 1.11V$	$V_{bi} = 0.52V$	$V_{bi} = 1.18V$
$N_d = 1.63 \cdot 10^{14}$	$N_d = 1.40 \cdot 10^{14}$	$N_d = 2.16 \cdot 10^{14}$	$N_d = 1.92 \cdot 10^{14}$

The value of V_{bi} has to be lower than the value of silicon band-gap, that is roughly 1.1V. Therefore the correct values of V_{bi} are the ones from *Region 1*.

As it can be observed in the $1/C^2$ plots, both gold and aluminum diodes show the same behavior but the step appears at different values of voltage. The steps are roughly 1V away. The idea is that the material of the contacts influences the measurement, and what we thought is that this difference is due to the difference in the work function of this metals. The work function values are 5.1 V for gold and 4.1 V for aluminium, so the difference is 1V, exactly the same value that has been obtained. Because of these results, it is reasonable to think that the materials chosen for the contacts play an important role.

B. Sweep frequency response

The frequency-dependency of the complex admittance of the solar cell can yield useful information about the junction.

The capacitance measures the mobile charge density within a small distance at the edge of the depletion width w (determined by the DC bias voltage V). Trapped charge can respond to low frequencies but not to high frequencies. Thus, traps contribute to the low-frequency capacitance, but not to the high-frequency capacitance [7].

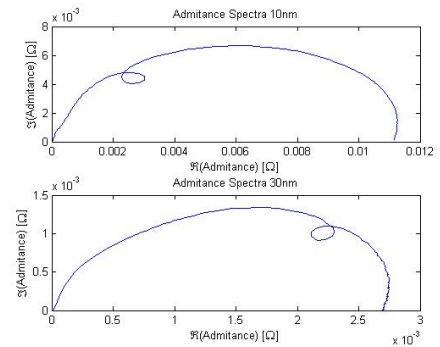


FIG. 6. Admittance Spectra for hybrid HIT solar cells with different thicknesses of MoO_3

The admittance is calculated for a model circuit consisting of two impedances in series, each of which is formed by a capacitance in parallel with a shunt resistance.

For the first impedance set, the capacitance is C and the shunt resistance is R_p ; for the second impedance set, the capacitance is C_x and the shunt resistance is R_x . In series with the two impedance sets, there is a third resistance, R_s , and finally an inductance, L . The inductance considered in this model is not an intrinsic parameter of the solar cell but a consequence of the wires connecting the solar cell to the measurement devices. In the measurements of conductance and capacitance, the effect of the inductance can be observed. In Figure 6 the loop that appears in the curve is due to LC resonance.

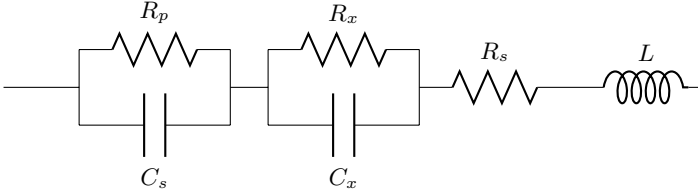


FIG. 7. Circuit model

The admittance is defined as the inverse of the complex impedance: $A(\omega) = 1/Z(\omega) = G_m(\omega) + j\omega C_m(\omega)$. From this value, the conductance and capacitance of the circuit can be extracted:

$$G_m(\omega) = \Re\{A(\omega)\} \text{ and } C_m(\omega) = \Im\{A(\omega)\}/\omega \quad (6)$$

The complex impedance of the circuit model in Figure 7 is:

$$Z(\omega) = R_s + j\omega L + \frac{R_p \frac{1}{j\omega C}}{R_p + \frac{1}{j\omega C}} + \frac{R_x \frac{1}{j\omega C_x}}{R_x + \frac{1}{j\omega C_x}} \quad (7)$$

In order to simplify the expressions, in the high frequency limit for the capacitance, C_m , one has to take the terms down to ω^4 . This approximation has been taken given the fact that the frequencies with which the data has been obtained are not high enough so as to not to consider this terms. On the other hand, for the conductance, due to the multiplicative terms one can consider not taking into account these terms in order to simplify the expressions and to be able to solve it.

$$G_m(\omega) = \begin{cases} \frac{1}{R_x + R_p + R_s} & , \omega \rightarrow 0 \\ \frac{R_s}{\omega^2 L^2} & , \omega \rightarrow \infty \end{cases} \quad (8)$$

and

$$C_m(\omega) = \begin{cases} \frac{-L + R_x \tau_x + R_p^2 C}{(R_x + R_s + R_p)^2} & , \omega \rightarrow 0 \\ \frac{-L \alpha^2}{(L \beta + R_s \alpha)^2 + L \alpha (\omega^2 L \alpha - 2(L + \tau_x R_p + R_s \beta + \tau_p R_x))} & , \omega \rightarrow \infty \end{cases} \quad (9)$$

with $\tau_x = C_x R_x$, $\tau_p = C R_p$, $\alpha = \tau_x \tau_p$ and $\beta = \tau_x + \tau_p$.

Obtaining a frequency sweep measure of the complex impedance of the solar cells and using the this formulas, the values of the components of the circuit model for each cell can be obtained. To simplify the procedure, the measurements were performed in the dark with cells in reverse bias (-2, -1, -0.5 and -0.1 V).

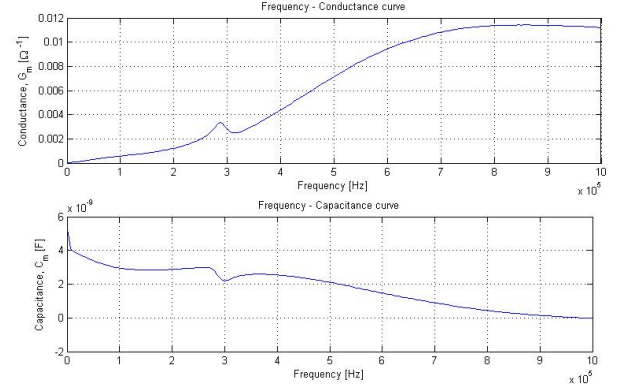


FIG. 8. Plot of the conductance and the capacitance as a function of the frequency for a 10nm hybrid HIT solar cell with a voltage of -0.1V

In order to solve the equations, the values for R_p and R_s are the ones found in the analysis for the IV curves. Therefore, one has 4 equations and 4 parameters to determine (L , C_x , R_x and C). Solving the equations using Matlab, the following values have been obtained for the different parameters:

	HIT 10nm	HIT 30nm	HIT 30nm	HIT 30nm
Voltage [V]	-1	-2	-1	-0.5
C [μF]	1.68	93.89	27.60	15.03
C_x [nF]	40.52	23.00	20.28	26.45
R_x [k Ω]	2.52	249.03	95.70	49.03
L [μH]	1.27	2.30	2.49	1.92

As it is expected and according to [7] the values of the inductance are small, which means that is an effect due to the wires.

VI. CONCLUSIONS

The results obtained for the Schottky diodes and the parameters of the hybrid HIT solar cells, as it has been already commented, do correspond with reality. In fact, the ideality factors and efficiencies calculated show a good behaviour of the hybrid HIT solar cells. However, the results obtained for the circuital model are not as accurate as it would be expected in spite of the fact that the order of magnitude is reasonable. When the admittance of the circuital model is plotted, important discrepancies with the measured values are observed. Therefore, further studies should be carried out.

-
- [1] Battaglia, Corsin and Yin, Xingtian and Zheng, Maxwell and Sharp, Ian D. and Chen, Teresa and McDonnell, Stephen and Azcatl, Angelica and Carraro, Carlo and Ma, Biwu and Maboudian, Roya and Wallace, Robert. M. and Javey, Ali. *Hole Selective MoOx Contact for Silicon Solar Cells*. Nano Letters 14.2 (2014): 967-71. Web.
- [2] Battaglia, Corsin and de Nicolas, Silvia Martin and De Wolf, Stefaan and Yin, Xingtian and Zheng, Maxwell and Ballif, Christophe and Javey, Ali. *Silicon heterojunction solar cell with passivated hole selective MoOx contact*. Applied Physics Letters, 104, 113902 (2014). Web
- [3] Spectra-Physics. *Manufacturing c-Si Solar Cells with Lasers*. Web.
- [4] Willis, Shawn. *Advanced Optoelectronic Characterisation of Solar Cells*. N.p.: Oxford U, 2011. Print.
- [5] Macabebe, Erees Q.B. and van Dyk, E. Ernest. (2008). *Parameter extraction from dark current-voltage characteristics of solar cells*. South African Journal of Science, 104(9-10), 401-404. Retrieved May 23, 2014, Web.
- [6] Brus, V.v., M. Zellmeier, X. Zhang, S.m. Greil, M. Gluba, A.j. Tfflinger, J. Rappich, and N.h. Nickel. *Electrical and Photoelectrical Properties of P3HT/n-Si Hybrid Organic-inorganic Heterojunction Solar Cells*. Organic Electronics 14.11 (2013): 3109-116. Web
- [7] Scofield, John H. *Effects of Series Resistance and Inductance on Solar Cell Admittance Measurements*. Solar Energy Materials and Solar Cells 37.2 (1995): 217-33. Web.